

Spin-density-wave clusters in PdMn spin-glass alloys

Y. Tsunoda and N. Hiruma

Department of Applied Physics, School of Science and Engineering, Waseda University, 3-4-1 Okubo, Shinjuku, Tokyo 169, Japan

J. L. Robertson and J. W. Cable

Solid State Division, Oak Ridge National Laboratory, Oak Ridge, Tennessee 37831

(Received 30 May 1997)

PdMn disordered alloys with concentrations above 5 at. % Mn display characteristic properties of spin glasses. We report here neutron-diffraction data for Pd₉₀Mn₁₀ and Pd₈₀Mn₂₀ single crystals. Satellite diffuse peaks were observed for both specimens at the $(1 \pm \delta 0 0)$ positions ($\delta=0.37$ for Pd₉₀Mn₁₀ and $\delta=0.16$ for Pd₈₀Mn₂₀) accompanied with the atomic-short-range-order peak at $(1 0 0)$. These satellites disappear at temperatures far above the freezing temperature T_f . The origin of the spin-glass-like behavior in PdMn alloys can be ascribed to the dynamics of the fluctuating spin-density-wave clusters just as observed in CuMn alloys. Various properties observed here are compared with those of CuMn alloys. [S0163-1829(97)03342-0]

I. INTRODUCTION

The magnetic phase diagram of the PdMn alloy is something extraordinary and has attracted the attention of many researchers. The PdMn alloy with Mn content below 5 at. % shows ferromagnetic behavior at low temperature, but the alloy with higher Mn content displays typical characteristics of a spin glass; a cusp-type anomaly and remanent magnetization in susceptibility measurements, but no obvious peak around the freezing temperature in the specific heat.^{1,2} This peculiar feature of the PdMn phase diagram is explained as a crossover of the indirect spin coupling through the Ruderman-Kittel-Kasuya-Yosida (RKKY) interaction and the direct Mn-Mn interaction. The former is predominant in the low-concentration alloy and stabilizes the ferromagnetic coupling between distant Mn atoms due to the spin polarization with strong enhancement in the Pd host just like the PdFe alloy. The latter favors antiferromagnetic coupling between the nearest-neighbor Mn pairs. Thus, the frustration between the indirect RKKY-type interaction and the direct Mn-Mn interaction plays a significant role in stabilizing the spin-glass phase.³ In this spin-glass phase, Morgownik *et al.* performed neutron-diffraction measurements using 9.96 at. % Mn polycrystal samples and observed rather strong magnetic correlations surviving even at room temperature.⁴ Saha *et al.* recently studied the atomic short-range order (ASRO) in various compositions of disordered PdMn alloys by electron and x-ray diffraction using single-crystal specimens. They pointed out that competing interactions between long-range ferromagnetic coupling and near-neighbor antiferromagnetic coupling play important role in understanding the spin-glass-like behaviors of this alloy.⁵

On the other hand, the alloys with Mn content around 25 at. % show the well-developed chemical order of Pd₃Mn and were more familiar research objects. Cable *et al.* studied the chemical order and magnetic structure for thermally treated Pd₃Mn alloys using polycrystalline samples.⁶ They observed a one-dimensional antiphase domain structure based on the Cu₃Au-type chemical order and antiferromagnetic long-range order. However, disordered alloys with roughly 25

at. % Mn still show spin-glass-like susceptibility. Rainford has studied magnetic scattering of neutrons using disordered Pd₇₅Mn₂₅ single crystals and found satellite diffuse peaks at $1 \pm \delta 0 0$ ($\delta=0.15$) developing below room temperature together with ASRO peaks located at the $1 0 0$ reciprocal lattice point (RLP). These satellite peaks survive far above the freezing temperature T_f (~ 30 K).⁷ These data seem to include most of the essential points in understanding a metallic spin glass. Unfortunately, since the data were taken for only one specimen and since the spin-density-wave (SDW) description for the typical spin glass alloy CuMn were not available at that time, he did not discuss the role of the SDW clusters as the origin of spin-glass-like behavior.

In the present paper, we report the experimental data of magnetic scattering of neutrons for Pd₉₀Mn₁₀ and Pd₈₀Mn₂₀ disordered alloy single crystals. At low temperature, we found diffuse satellite reflections for both specimens. The satellite peaks are located at the $1 \pm \delta 0 0$ positions on the $[100]$ axis and the equivalent symmetry positions. The satellite peak position parameter, δ , varies with Mn concentration. The satellite peak intensity disappears at a far higher temperature than the freezing temperature at which the cusp-type anomaly is observed in the susceptibility measurements. Various features observed here are very similar to those observed in the typical spin-glass alloy CuMn. We compare the experimental results of these systems and discuss the origin of the spin-glass-like behavior of this system on the basis of dynamically fluctuating SDW clusters just as observed in CuMn spin-glass alloys.

II. EXPERIMENT

Single-crystal specimens with Mn content of 10 and 20 at. % were grown in Al₂O₃ crucibles using a furnace with a carbon heater system in an Ar atmosphere. Both specimens have a volume of roughly 1 cc and were used for neutron-scattering measurements in the as-grown state. A small piece of crystal was cut from each single-crystal ingot for the purpose of susceptibility measurements. Neutron-scattering measurements were carried out at the HB-1A triple axis

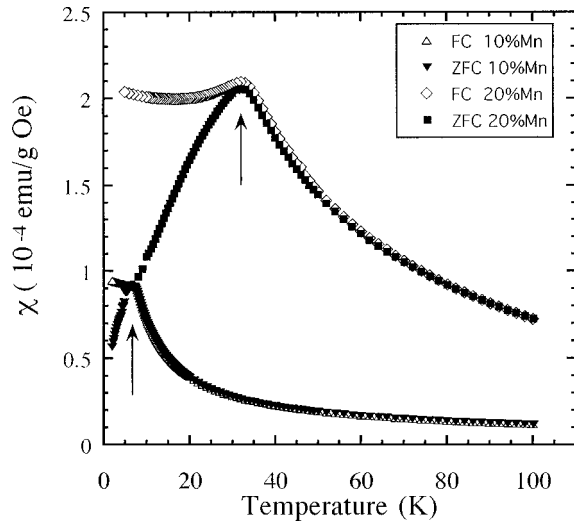


FIG. 1. Susceptibility data studied for the specimens cut from each single crystal for neutron scattering.

spectrometer at the high-flux-isotope reactor, Oak Ridge National Laboratory, and part of the data were taken at the T1-1 triple axis spectrometer installed at a thermal guide of JRR-3M, Tokai.

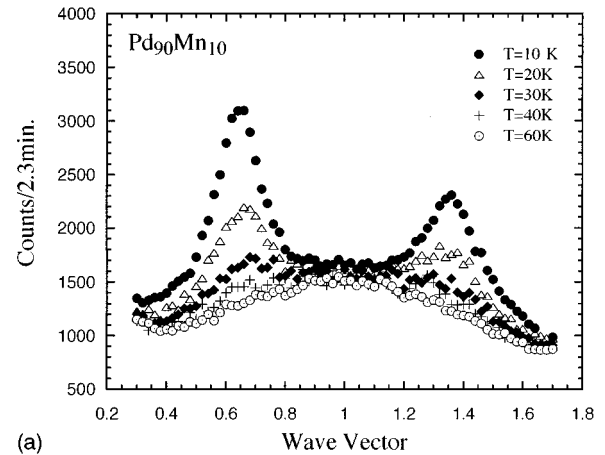
Most of the data were taken in the elastic setting using analyzer crystals. The energy resolution of the present experimental condition is estimated to be 0.7 meV in full width at half maximum, indicating that the spin dynamics moving slower than 2×10^{11} Hz is observed as elastic scattering.

Susceptibility measurements were carried out using a superconducting quantum interference device (SQUID) system at the Materials Characterization Central Laboratory, Waseda University, in the temperature range between 1.6 and 110 K.

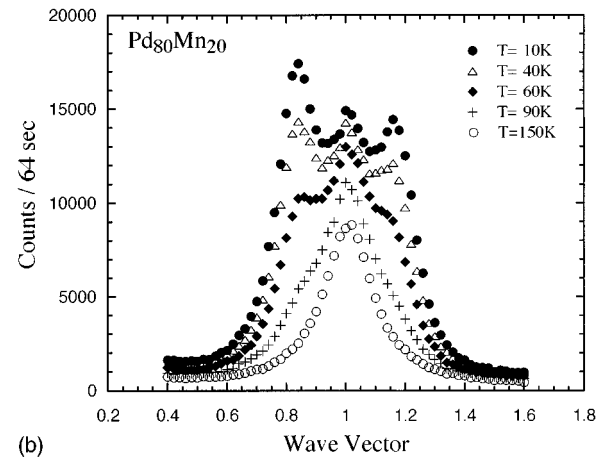
III. EXPERIMENTAL DATA

A. Susceptibility

In order to confirm that our specimens show spin-glass-like behavior, we performed the susceptibility measurements using the specimens cut from each single crystal for neutron-scattering measurements. A SQUID magnetometer was used and data were taken in a magnetic field of 100 G. Experimental data are depicted in Fig. 1. Both samples actually show a typical spin-glass behavior; a cusp-type peak at the freezing temperature T_F and remanent magnetization below T_F . The freezing temperatures of these specimens are esti-



(a)



(b)

FIG. 2. (a) Diffraction line profiles observed at various temperatures for $\text{Pd}_{90}\text{Mn}_{10}$. The data were taken by scanning along the $[1\ 0\ 0]$ axis. (b) The experimental data studied at various temperatures for $\text{Pd}_{80}\text{Mn}_{20}$.

mated to be 7 and 31 K for $\text{Pd}_{90}\text{Mn}_{10}$ and $\text{Pd}_{80}\text{Mn}_{20}$ alloys, respectively. These values are consistent with those published by previous authors.⁵ Thus, although our samples have no thermal treatment (furnace cooled), magnetic behavior in the susceptibility measurements look like the typical spin-glass system.

B. Neutron diffraction

The diffraction patterns observed at various temperatures for $\text{Pd}_{90}\text{Mn}_{10}$ are given in Fig. 2(a) and those for the $\text{Pd}_{80}\text{Mn}_{20}$ alloy are given in Fig. 2(b). These data were taken

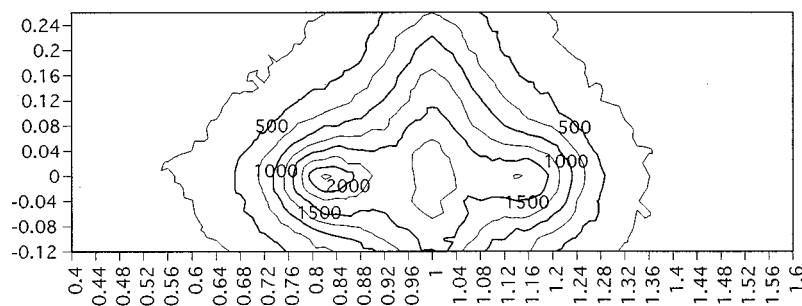


FIG. 3. Scattering intensity contour map around the $1\ 0\ 0$ RLP studied at 10 K for $\text{Pd}_{80}\text{Mn}_{20}$.

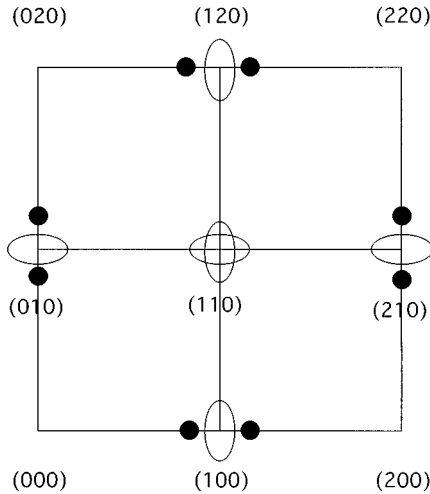


FIG. 4. Closed circles; observed satellite peak positions on the (001) scattering plane. Open ellipsoid; ASRO peak positions.

by scanning along the $[100]$ axis around the 100 reciprocal lattice point. Both show satellite peaks at $1 \pm \delta 00$ positions in addition to the peak at the 100 RLP. The 100 peak studied at 60 K for Mn 10% is very weak and broad. Since the 100 peak intensities for both specimens are temperature-independent, these are considered to be atomic in origin. We will discuss this point later. The satellite peaks are temperature-dependent and are considered to be magnetic reflections. An asymmetric intensity for the two satellite peaks is probably due to the wave vector dependence of the magnetic form factor and this also supports a magnetic origin. Two-dimensional intensity distribution around the 100 RLP was also studied for the Mn 20% alloy and the observed intensity contour map is given in Fig. 3. The satellite peaks are located on the $[100]$ axis and the intensity distribution of the satellite peak is almost isotropic. However, the intensity distribution of the 100 peak has a different shape from those of the satellites; the scattering intensity elongates along the $[010]$ axis. This is consistent with the electron-diffraction data studied by Saha *et al.*⁵ All of the satellite peak positions observed on the (001) plane are illustrated in Fig. 4. Note that the satellite peaks are observed at the symmetry positions of a fcc lattice in the reciprocal space.

The temperature variations of the satellite peak intensities for both specimens are given in Fig. 5. In this figure, the arrows indicate the temperatures at which the cusp-type anomaly is observed in the susceptibility measurements. The satellite peaks disappear at temperatures far above the freezing temperature T_F and no anomaly of the intensities are observed at the freezing temperature. The temperature dependence of the satellite peak positions (Q) and the linewidth, which are determined from a Lorentzian fitting of the diffraction line profiles, are plotted in Figs. 6(a) and 6(b), respectively. The satellite peak positions for the Mn 20% alloy shift slightly towards the 100 RLP and the linewidth increases above the freezing temperature.

IV. DISCUSSIONS

PdMn has been considered to be an example of non-RKKY spin glass.³ However, we observed satellite reflec-

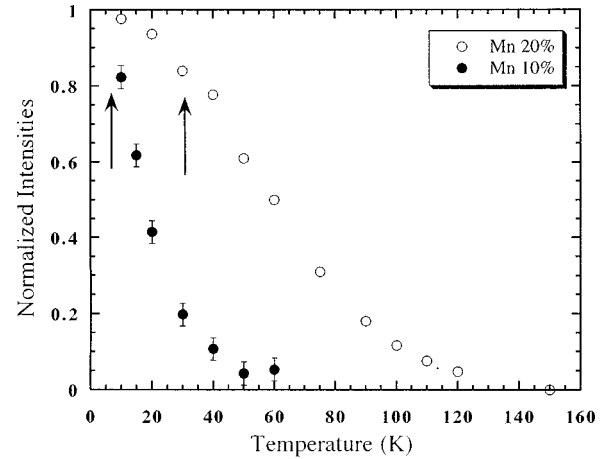


FIG. 5. The temperature variations of the $1-\delta 00$ satellite peak intensities for both specimens. The arrows indicate the freezing temperatures determined from the susceptibility data.

tions around the $1 \pm \delta 00$ positions, indicating that the spins have antiferromagnetic correlations and the spin structure is modulated along the $[100]$ axis. The wavelength estimated from the satellite peak position is about 3 times the lattice parameter for $\text{Pd}_{90}\text{Mn}_{10}$. The linewidth of the satellite peaks is far broader than that of the 200 Bragg reflection. The

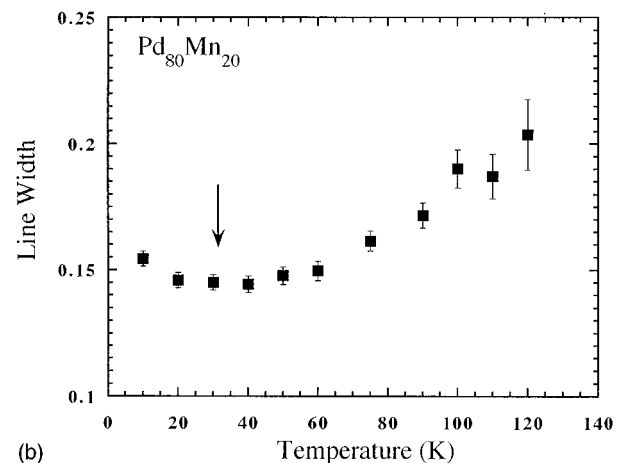
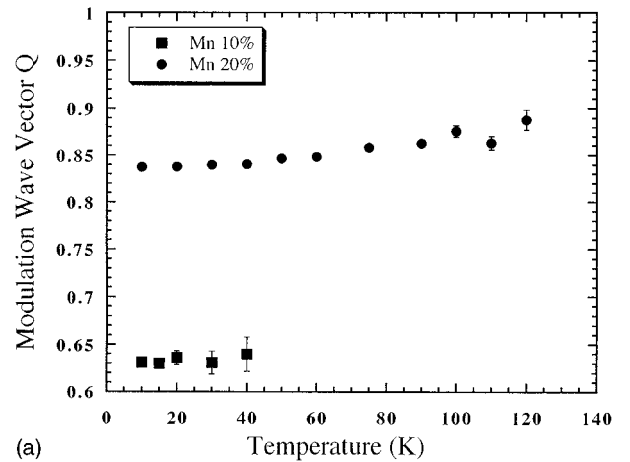


FIG. 6. (a) Temperature variations of the SDW wave vector Q for both specimens. (b) Temperature variation of the satellite linewidth for $\text{Pd}_{80}\text{Mn}_{20}$ alloy.

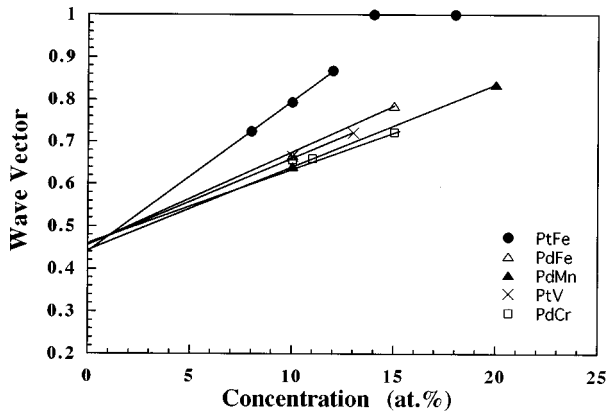


FIG. 7. The modulation wave vectors for various Pd-M and Pt-M (M:3D element) alloys determined from neutron-scattering data.

correlation length of spin modulation is estimated to be 7 times the lattice parameter for the Mn 20% alloy and 4~5 times for Mn 10% alloy. Thus the modulated spins form clusters with the size of roughly $15 \text{ \AA} \sim 27 \text{ \AA}$. The satellite peaks disappear far above the freezing temperature determined from the susceptibility measurements. In the latter, the response is observed for the uniform and static magnetic field. In neutron-scattering experiments, however, spin dynamics are observed through a window of the instrumental resolution. In the present case, since the energy resolution is about 0.7 meV, which corresponds to 2×10^{11} Hz, slow motions of the spin clusters are still observable as elastic scattering through the resolution window. Thus, even above the freezing temperature, the spin clusters fluctuate dynamically in keeping with the modulated spin correlation because the satellite reflections retain their line profiles. As clearly observed in CuMn alloys, spin-glass alloys show a different response depending on the frequency the experiment is operated.⁸

The modulated spin structure of PdMn seems to arise from a Fermi-surface effect for the following reasons: (1) The modulation wave vector Q ($|Q| = 1 - \delta$) varies continuously with the Mn concentration; (2) we observed diffuse satellite reflections at the same symmetry positions for PdCr (spin glass)⁹ and PdFe (ferromagnet)¹⁰ alloys with roughly the same solute compositions; (3) we observed also the diffuse satellite reflections at the same symmetry positions for PtFe (ferromagnet)¹⁰ and PtV (Ref. 11) (concentration wave) alloys and it is known that Pt and Pd have almost the same shaped Fermi surfaces;¹² (4) The extrapolations of the wave vector Q to zero solute concentration for these PdM and PtM (M; 3d-element) converge into the q value of about 0.45 ($2\pi/a$ unit) or 0.72 \AA^{-1} as shown in Fig. 7. In the Fermi surface of Pd, there exist parallel planes with a distance of about 0.4 around the W point. These surfaces are a good candidate of the Fermi surfaces satisfying the nesting condition. Since these are hole surfaces, increasing the Mn concentration leads to the expansion of the hole surfaces resulting in an increase of the Q value. This is consistent with the observation.

Therefore the modulated spin structure of the PdMn alloy is considered to be a spin-density wave based on nesting Fermi surfaces. Then the origin of the spin-glass-like behav-

ior in PdMn alloys is ascribed to the dynamics of the SDW clusters. When the correlation length of the incommensurate SDW becomes short, the frustration between the SDW clusters would be large because there are almost infinite freedoms in choosing the SDW phases. Thus, the SDW clusters fluctuate dynamically with various frequencies in a wide temperature range. This mechanism produces superparamagnetic SDW clusters with various frequencies. The line broadening below and above T_F would be explained by this mechanism. [See Fig. 6(b)]. There may be another mechanism based on the virtual bound state picture. The random distribution of solute atoms leads to ill-defined Fermi surfaces, resulting in the ill-defined SDW with short lifetimes. These pictures for the spin-glass alloys are just the same as those reported in typical spin-glass alloys CuMn (Ref. 3) and compelled us to study inelastic scattering of neutrons for this system. We observed strong inelastic scattering at the satellite peak positions at far above T_F . This is again the same as the CuMn spin-glass alloys.¹⁴ The results of inelastic scattering will be published separately.¹⁵

The satellite peak positions for the Mn 20% alloy specimen shift slightly inwards at high temperature. This type of temperature variation has never been observed for CuMn spin-glass alloys,¹³ but is rather familiar for the SDW system originating in the Fermi-surface nesting such as Cr. The linewidth of the satellite peaks increases above the freezing temperature as observed in CuMn.¹³

The ASRO of PdMn alloys were studied by several authors using neutron, electron, and x-ray diffraction.^{4,5,16} All of the data seem to be qualitatively consistent; Warren-Cowley ASRO parameter α_1 is negative and α_2 has positive value, indicating that the unlike atoms prefer nearest-neighbor positions but like atoms prefer second-neighbor sites. Thus, the ASRO peak is observed at the 100 RLP, which is different from the magnetic satellite peak position $1 \pm \delta 00$. Furthermore, the linewidth of the ASRO peak for the Pd₉₀Mn₁₀ alloy is far broader than that of the magnetic satellite peaks. It should be pointed out that the CuMn alloy is another example of a system for which the ASRO and magnetic short-range order (SRO) have different symmetry.

In the CuMn alloy, the ASRO peak is observed at the $1 \frac{1}{2} 0$ RLP, but the magnetic SRO satellite peaks are observed at the $1 \pm \delta 10$ and $1 \pm \delta 0$ positions.¹³ Recently, the present authors found that the strong magnetic satellite peaks arise from the domains with well-developed ASRO for the Cu₆₅Mn₃₅ alloy.¹⁷ In that case, the satellite and ASRO peaks had similar line profiles. However, for low Mn concentration alloys ($C \sim 1.4$ at. %), the line profiles of magnetic satellite peaks and the ASRO peak are completely different.¹⁸ This situation is again similar with the case of PdMn alloys. The SDW seems to have nothing to do with the ASRO for the low-concentration alloys. In other words, the ASRO is not solely determined from the nesting energy of the Fermi surfaces for these alloys. This point should be compared with the PtV alloy. Very recently, we found temperature-independent diffuse satellite reflections at the same symmetry positions. $1 \pm \delta 00$ for Pt_{1-x}V_x ($x = 0.07, 0.10, \text{ and } 0.13$) alloys and the modulation vector δ again depends sensitively on the V concentration.¹² Since the PtV alloys in these compositions are nonmagnetic alloys, these satellite peaks are atomic in origin. A concentration wave of the constituent

atoms develops in the PtV alloy and this is probably due to the nesting Fermi surfaces.

The difference of these systems may be related to the atomic volume of the constituent atoms. The satellite peak intensities in the PtV alloy is strongly asymmetric, indicating that the concentration wave in the PtV alloy is accompanied by lattice distortions; the region with higher Pt concentration has an expanded lattice spacing. On the other hand, in CuMn and PdMn alloys, the solute atoms are considered to have larger volumes than the host atoms because the lattice parameters increase with increasing Mn content.

Except for the satellite peak positions, both PdMn and CuMn systems display almost the same behavior in neutron-scattering experiments. We can conclude that the origin of the spin-glass-like behavior for both systems is just the same; dynamically fluctuating SDW clusters. Until now, CuMn and AgMn were known as special metallic spin-glass systems with fluctuating SDW clusters. However, the present data verify that the PdMn and PdCr (and PtMn also) belong to the

same category. Thus, the dynamically fluctuating SDW clusters are a more common mechanism for the metallic spin-glass systems. Differences of these systems are that (1) the propagation directions of the SDW are different due to the difference of the Fermi surfaces of the host metals, and (2) there is a ferromagnetic phase in the PdMn alloy with low Mn concentration. The latter may be related to the strong enhancement of the susceptibility of pure Pd. Neutron-scattering measurements for the Pd₉₇Mn₃ ferromagnetic alloy are now being planned.

ACKNOWLEDGMENTS

The main part of present research was carried out at the Oak Ridge National Laboratory under the U.S.-Japan Cooperation Programme in Neutron Scattering, and was sponsored in part by the U.S. Department of Energy under Contact No. DE-AC05-96OR22464.

¹B. R. Coles, H. Jamieson, R. H. Taylor, and A. Tari, *J. Phys. F* **5**, 565 (1975).

²S. C. Ho, I. Maartense, and Gwyn Williams, *Phys. Rev. B* **24**, 5174 (1981).

³The data published before 1980 were reviewed by J. A. Mydosh and G. J. Nieuwenhuys, in *Ferromagnetic Materials*, edited by E. P. Wohlfarth (North-Holland, Amsterdam, 1980), Vol. 1, p. 2.

⁴A. F. J. Morgownik, G. J. Nieuwenhuys, J. A. Mydosh, and C. van Dijk, *J. Phys. F* **17**, 199 (1987).

⁵D. K. Saha, K. Ohshima, M. Y. Wey, R. Miida, and T. Kimoto, *Phys. Rev. B* **49**, 15 715 (1994).

⁶J. W. Cable, E. O. Wollan, W. C. Koehler, and H. R. Child, *Phys. Rev.* **128**, 2118 (1962).

⁷B. D. Rainford, *J. Magn. Mater.* **14**, 197 (1979).

⁸S. A. Werner, *Comments Condens. Matter Phys.* **15**, 55 (1990).

⁹M. Hirano and Y. Tsunoda (unpublished).

¹⁰Y. Tsunoda and R. Abe, *Phys. Rev. B* **55**, 11 507 (1997).

¹¹O. K. Andersen and A. R. Mackintosh, *Solid State Commun.* **6**, 285 (1968).

¹²A. Murakami and Y. Tsunoda (unpublished).

¹³J. W. Cable, S. A. Werner, G. P. Felcher, and N. Wakabayashi, *Phys. Rev. B* **29**, 1268 (1984).

¹⁴Y. Tsunoda, N. Kunitomi, and J. W. Cable, *J. Appl. Phys.* **57**, 3753 (1985).

¹⁵J. W. Cable, L. Robertson, N. Hiruma, and Y. Tsunoda (unpublished).

¹⁶N. Ahmed and T. J. Hicks, *J. Phys. F* **4**, L124 (1974).

¹⁷Y. Tsunoda and J. W. Cable, *Phys. Rev. B* **46**, 930 (1992).

¹⁸J. W. Cable and Y. Tsunoda, *J. Appl. Phys.* **73**, 5454 (1993).